Decoding the Ophthalmology Note: Understanding Clinical Symptoms and Physical Examination Findings in the Context of Imaging Pathology

B.M. Cavazuti, V.H. Chen, A.H. Aiken, K.M. Narayana, and A. Corey

CME Credit

The American Society of Neuroradiology (ASNR) is accredited by the Accreditation Council for Continuing Medical Education (ACCME) to provide continuing medical education for physicians. The ASNR designates this enduring material for a maximum of one AMA PRA Category one credit™. Physicians should claim only the credit commensurate with the extent of their participation in the activity. To obtain credit for this activity, an online quiz must be successfully completed and submitted. ASNR members may access this quiz at no charge by logging on to eCME at http://members.asnr.org. Nonmembers may pay a small fee to access the quiz and obtain credit via http://members.asnr.org/ecme.

ABSTRACT

Orbital and visual pathway pathology often leads to readily apparent symptoms and physical examination findings. Although in-office testing does provide clues to the underlying problem, further diagnostic workup and confirmatory imaging tests may be necessary. For the interpreting radiologist to use the correct protocol for a study and to tailor an appropriate differential diagnosis, a basic understanding of the ophthalmology note, anatomy of the eye and visual apparatus, and the more common ophthalmologic concerns is crucial. The purpose of this review was to provide the radiologist with the ophthalmologist's perspective on abnormalities of the eye and vision, supplemented by correlative clinic notes and imaging examples.

Learning Objective: Review the critical portions of the ophthalmologic examination and in-office tests, their documentation, and how these data may be used for enhancing image interpretation.

INTRODUCTION

This article reviewed the critical portions of the ophthalmologic examination and in-office tests, their documentation, and how these data may be used for enhancing image interpretation. Evaluation of visual acuity, visual field testing, pupillary response, extraocular muscle (EOM) function, and assessment of the globe are presented, with a focus on what the neuroradiologist needs to know. Illustrative case examples are provided to reinforce the correlation with key portions of the ophthalmologic examination and clinical note.

ANATOMY OF VISION

The bony orbit is made up of 7 bones: the frontal bone superiorly, lacrimal bone, ethmoid bone and nasal bone medially, maxillary bone medially and inferiorly, zygomatic bone inferiorly and laterally, and sphenoid bone posteriorly. The orbit itself is divided into 3 compartments: the muscle cone, which consists of all intraocular muscles except the inferior oblique muscle; the intra- and extraconal spaces; and the globe. The globe is in continuity with the central nervous system via the optic nerve and is made up of 3 layers: the sclera, uvea, and retina. The

ABBREVIATION KEY

CN = cranial nerve
EOM = extraocular muscle

Received February 10, 2016; accepted November 8, 2016.

From the Department of Radiology and Imaging Sciences (B.M.C.), Department of Ophthalmology (V.H.C.), Department of Radiology and Imaging Sciences, Division of Neuroradiology (A.H.A., A.C.), and Department of Ophthalmology, Division of Neuro-ophthalmology (K.M.N.), Emory University School of Medicine, Atlanta, Georgia.

Previously presented as an educational exhibit at: Annual Meeting of the American Society of Head and Neck Radiology, September 9–13, 2015; Naples, Florida.

Please address correspondence to Bethany Milliron Cavazuti, MD, Department of Radiology and Imaging Sciences, Emory University School of Medicine, 329 Patterson Way NE, Atlanta, GA 30312; e-mail: bmcavazuti@gmail.com

http://dx.doi.org/10.3174/ng.3170201

Disclosures
Based on information received from the authors, *Neurographics* has determined that there are no Financial Disclosures or Conflicts of Interest to report.

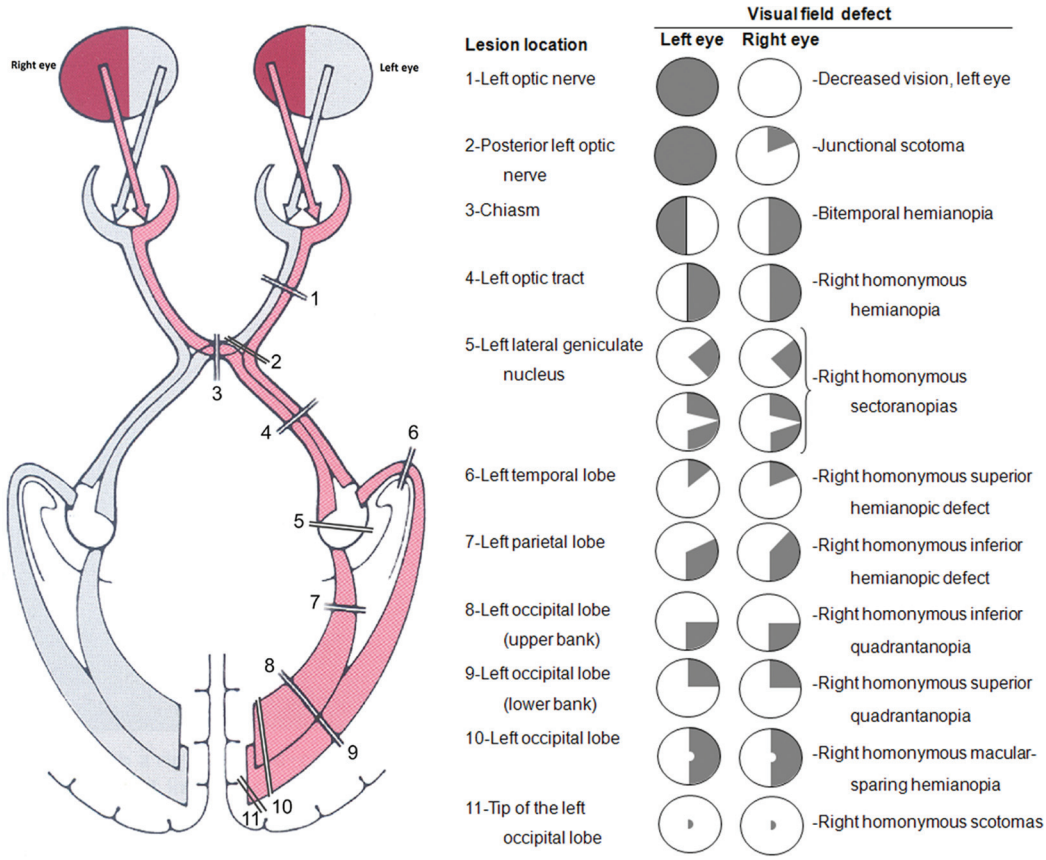

Fig 1. Visual field defects. Visual field defects will vary in size, shape, location, and laterality, depending on their location along the visual axis. This diagram demonstrates the complexity of visual field defects and their diagnosis. Used with permission of Valerie Biousse, MD, and Nancy J. Newman, MD, and Thieme Publishing (Ref. 6, Fig 5.1).

sclera is the outermost layer and consists of collagenous tissue. The sclera is continuous anteriorly with the transparent cornea and posteriorly with the dura mater. The uvea is the middle layer and consists of the iris, ciliary body, and choroid. The retina is the innermost layer and is the light sensitive part of the eye, continuous posteriorly with the optic nerve.[1]

The globe can be further compartmentalized into 2 segments: the anterior segment and the posterior segment.[1] The anterior chamber and the posterior chamber together make up the anterior segment. The anterior chamber margins are the posterior aspect of the cornea anteriorly, the anterior aspect of the iris and lens posteriorly, and the drainage angle laterally. The posterior chamber is the space from the posterior surface of the iris to the anterior surface of the zonular fibers, bordered laterally by the ciliary processes. The anterior portion of the posterior segment is formed by the zonular fibers, ciliary body, and the posterior aspect of the lens. The posterior portion is formed by the optic nerve and the retina.[2] The visual pathway extends from the eyes to the occipital lobes (Fig 1). In brief, the pathway begins at the retina and travels posteriorly via the optic nerve, decussating at the optic chiasm, continuing posteriorly along the optic tract to the lateral geniculate nucleus, then radiating through the temporal and parietal lobes, and finally reaching the occipital lobe.

OPHTHALMOLOGY NOTE AND PHYSICAL EXAMINATION

An example of an ophthalmology note template used in our medical system is shown in Fig 2. Ophthalmologic clinical note templates vary widely among institutions and even among physicians at the same institution; however, the abbreviations and diagrams used by ophthalmologists to document their findings are standardized to a significant extent. Although the ophthalmology note may not always be available at the time of imaging interpretation, referring ophthalmologists do provide clinical histories on the imaging order that reference clinical examination findings by using vocabulary unique to this specialty. Radiologists should be familiar with common abbreviations in the ophthalmology note, such as OD for right eye and OS for left eye, with additional examples listed in Table 1.

Ophthalmologists use common tests to assess the anatomy and function of the ocular apparatus. An anatomic examination of the eye starts externally with the lid and adnexa, and moves internally with the aid of a slit lamp for anterior segment and an ophthalmoscope and stereoscopic methods for evaluation of the fundus. Ocular motility and pupillary responses are other important clinical evaluations. Visual field testing and the use of an Amsler grid assess the fields and qualitative aspects of vision. The relative globe position and proptosis are assessed with an ex-

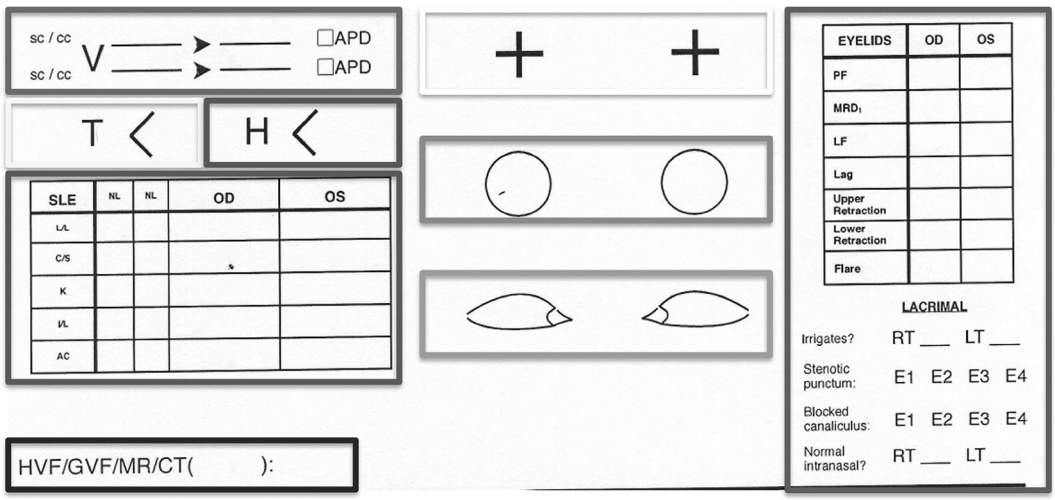

Fig 2. An example of an ophthalmology clinical note template. This template contains various components of the ophthalmologic examination to allow for ease of charting in a busy clinical setting. The top left box contains the evaluation of visual acuity (including without a pinhole more than with a pinhole, if used to correct for refractive error) and assessment for afferent pupillary defect (APD). Immediately below this is the area for assessment of intraocular pressure with a Tono-Pen (T) and evaluation of exophthalmos with a Hertel exophthalmometer (H). The third left box is the area for documenting the SLE, and the bottom left box is where visual field testing results (HVF/GVF) and imaging findings (MR and/or CT) are recorded. The top box in the middle row denotes the area for recording extraocular motility (+); below that is the area for recording lid position, scleral show, and corneal pathology; and the bottom box in the middle row is where evaluation of the lens, sclera, or conjunctiva are recorded. Finally, evaluation of the lids and adnexa are recorded on the far right. PF indicates palpebral fissure; MRD1, margin-reflex distance to evaluate for ptosis; LF, levator function; and Flare, the ability to see the light beam as it passes through the aqueous humor.

ophthalmometer, and intraocular pressure is measured with a tonometer. In-office B-scan ultrasonography can be supplemental to interrogate the vitreous and retina when the view to the fundus is obscured by media opacity such as an attenuated cataract or vitreous hemorrhage.

OVERVIEW OF IMAGING MODALITIES

Much of the eye and the visual axis can be assessed clinically; therefore, imaging is used judiciously to target a specific diagnostic question provoked by abnormal or unexplained examination findings. The choice of imaging technique, CT versus MR imaging, depends on the acuity of the situation and the specific pathology being evaluated. MR imaging is typically the test of choice for most neuro-ophthalmologic concerns (see Table 2 for 5 neuro-ophthalmologic emergencies that warrant imaging); however, CT is preferred in the setting of emergent scans, acute hemorrhage, evaluation of calcifications, osseous pathology, or trauma, or when MR imaging is precluded by the patient's condition.[3]

DECREASED VISUAL ACUITY, ABNORMAL COLOR VISION, AND VISUAL FIELD DEFECTS

Ophthalmologic Examination

The most important portions of the history in the ophthalmologic evaluation of a patient with vision loss are establishing timeline of vision loss and defining whether the defect is monocular or binocular. Visual acuity is readily tested by using a Snellen chart. Normal vision is recorded as 20/20, which means that the test subject sees the same line of letters at 20 feet that a subject with "perfect vision" sees at 20 feet. Decreased visual acuity, for example, 20/40, means that the patient sees at 20 feet what a normal subject is able to see from a greater distance (40 feet in this case). If the 20/400 line cannot be read, then the ability to count fingers (CF), hand motion perception (HM), light perception (LP), or no light perception (NLP) is recorded. The most common causes of decreased visual acuity worldwide are uncorrected refractive errors, followed by cataracts.[4] Testing is usually performed without and with the use of pinholes. If vision improves when viewing the Snellen chart through the pinholes, then the acuity issue is most likely related to a refractive problem.

Evaluation of vision also includes the assessment of color vision, which is commonly tested by using Ishihara color plates (Fig 3). Color vision deficiency can be congenital or acquired. Dyschromatopsia (a defect in color vision) is a particularly important clinical sign of optic nerve disease.[5] Charting of visual field testing is unique in that it is recorded from the patient's perspective, as if the clinician were seeing through the patient's eyes with the left eye on the left and the right eye on the right (Fig 4). The remainder of the eye examination is documented as the examiner is looking at the patient with the left eye on the right and the right eye on the left. In the diagrammatic representations of the visual field, the darkened portion represents where the patient has decreased or lost vision.

An Amsler grid, which resembles a piece of graph paper, is used to test for abnormalities of the retina and the posterior visual pathway, specifically those abnormalities that affect the central and paracentral vision. Confrontation visual field testing (CVF) grossly evaluates the central 30° of vision. This is performed with the examiner standing oppo-

Table 1: Common ophthalmology abbreviations

Abbreviation	Meaning
OD	Oculus dexter, or right eye
OS	Oculus sinister, or left eye
OU	Oculus uterque, or both eyes
BCVA	Best corrected visual acuity
Sc	Sine correctione, or without correction
Cc	Cum correctione, or with correction
CL	Contact lens
rAPD	Relative afferent pupillary defect
CF	Count fingers
HM	Hand motion
LP	Light perception
NLP	No light perception
CVF	Confrontation visual field
GVF	Goldmann visual field
HVF	Humphrey visual field
SLE	Slit lamp examination
L/L	Lids/lashes
C/S	Conjunctiva/sclera
K	Cornea
I/L	Iris/lens
IOL	Intraocular lens
PCIOL	Posterior chamber intraocular lens
AC	Anterior chamber
DFE	Dilated fundus examination

Table 2: A helpful mnemonic for 5 neuro-ophthalmologic emergencies that warrant imaging: the 5 A's

Etiology	Signs/Symptoms
Aneurysm	Acute CN III palsy
Apoplexy	Headache in combination with CN II or III palsy
Arterial dissection	Acute neck pain or headache; with or without Horner syndrome or stroke-like symptoms
Angioinvasive (ie, fungal infections)	Orbital or cavernous sinus symptoms (proptosis, ptosis, lid changes, optic neuropathy, motility defects, or other cranial neuropathies)
Arteritis (giant cell or temporal)	New-onset headache, vision loss, or motility changes in patients ages > 55 y

Note:—CN indicates cranial nerve.

site the patient while the patient maintains central fixation (eg, on the examiner's nose) as fingers are presented in the periphery, testing each eye individually (Fig 5). Other methods for evaluation of the visual fields include Humphrey visual field testing (HVF), which is an automated method that randomly tests points within the central visual field (24° or 30° tested monocularly) and Goldmann visual field testing (GVF), which is an examiner-dependent method to chart the entire visual field and is best suited for ill, poorly attentive, very young and very elderly patients, or patients with decreased vision (<20/100).

Imaging

Vision changes and visual field defects can vary, depending on the site of injury along the visual pathway; various deficits can be seen unilaterally or bilaterally, and the specific nature of the defects commonly have a useful role in localizing lesions (Fig 1) and thus in guiding imaging technique and coverage choices.

ABNORMAL VISION: MONOCULAR

Monocular defects localize anterior to the chiasm. The differential diagnosis for monocular vision loss includes pathology of the eye and optic nerve, including corneal disease; anterior chamber infection or hemorrhage, cataract, or lens dislocation; vitreous infection or blood; choroidal or retinal detachment; retinopathy; or optic neuropathies.[6] Masses such as meningiomas and orbital neoplasms that compress the optic nerve can cause optic neuropathy and vision loss. Age-related macular degeneration, glaucoma, and optic nerve damage are common causes of permanent vision loss.[4] In some instances, these monocular lesions will cause a unilateral visual field defect that respects the horizontal meridian as in the setting of altitudinal defects found in ischemic optic neuropathy. An optic nerve lesion typically affects the central 30° of the visual field (Fig 1).[6]

Optic neuritis is another cause of monocular (and sometimes binocular) vision loss. These patients often present with acutely decreased visual acuity, abnormal color vision, and painful eye movements,[7] as in the patient documented in Fig 6. Such inflammation of the optic nerve may be an initial manifestation of multiple sclerosis[6,8] Although optic neuritis is a clinical diagnosis in most cases, MR imaging can be useful to assess the optic apparatus and evaluate for associated demyelinating brain lesions.[9] Typical MR imaging findings of acute optic neuritis, including an enlarged, T2 hyperintense, and enhancing optic nerve are also demonstrated in Fig 6.[10] Optic nerve inflammation can be demonstrated on contrast-enhanced MR imaging in approximately 95% of patients with active optic neuritis.[6] MR imaging findings of chronic optic neuritis include increased T2-weighted signal intensity in an atrophic and nonenhancing optic nerve.[10] In patients with subacute to chronically decreased vision, evaluation for other inflammatory and neoplastic processes, such as idiopathic orbital inflammation, optic nerve glioma, or optic nerve sheath meningioma, should be pursued. For assessment of monocular vision loss, MR imaging of the orbit is the preferred imaging.[6]

ABNORMAL VISION: BINOCULAR

The etiology of binocular field defects is broad. Binocular field defects can be the result of bilateral globe or prechiasmatic lesions (such as in the setting of bilateral optic neuritis), intracranial pathology that affects the chiasmatic or

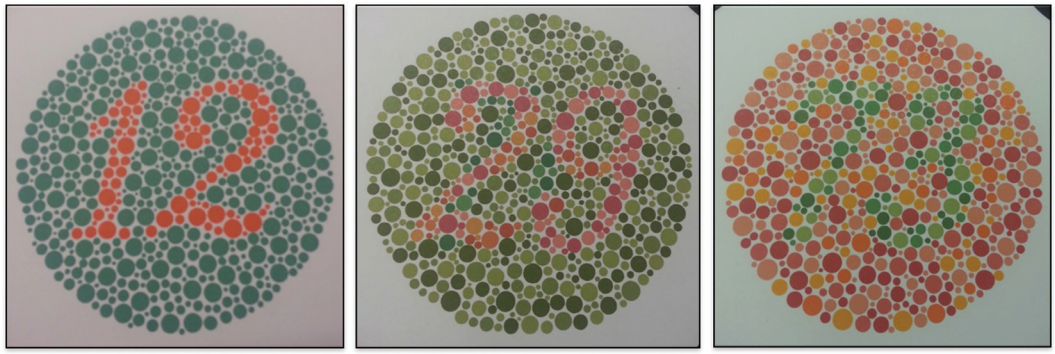

Fig 3. Ishihara color plates. Evaluation of color vision is part of the visual acuity assessment. Nine, 11, or 14 Ishihara color plates, each with varying levels of contrast between dots, which create numbers, and surrounding background are shown to the patient. Plates 1 through 11 evaluate for red-green color blindness with plates 12 through 14 further differentiating an abnormal result. A score of 10 –11 correct of 11 is a normal result, whereas 1–7 correct would be considered abnormal.

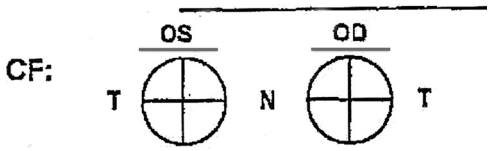

Fig 4. Visual field testing. Visual fields are recorded with right eye (OD) on the right and left eye (OS) on the left, as if the physician is seeing through the patient's eyes. Note the change compared with other parts of the ophthalmology chart (ie, fundoscopic examination), which are documented as if looking at the patient. Note:—n indicates nasal; T, temporal aspects of the visual field.

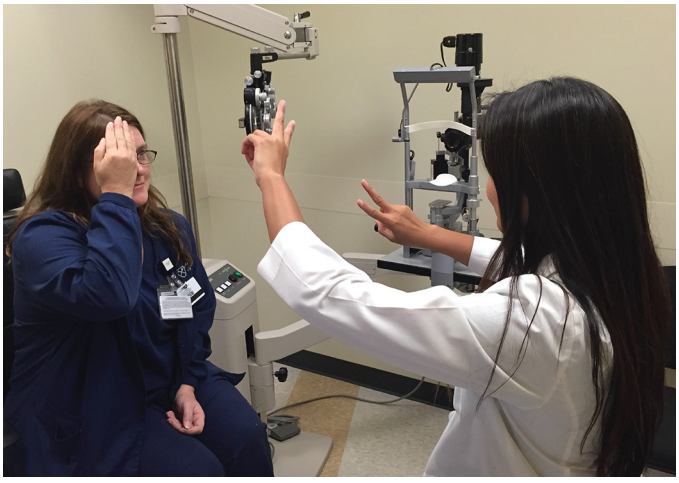

Fig 5. An example of confrontational visual field testing.

postchiasmatic visual pathway, or systemic conditions. For example, in patients with diabetes, visual acuity can be decreased transiently secondary to acutely increased blood glucose, with subsequent osmotic swelling of the lens, which results in a temporary myopia, or is permanently related to diabetic retinopathy.[4] If binocular visual field defects are present, then it is important to see if one or both defects respect the vertical. Even if one field respects the vertical meridian, the lesion is at or behind the chiasm,[4] as shown in Fig 1. Depending on the nature of the defect, imaging could include dedicated views of the orbits or sella in addition to the brain.

The classically described visual field defect of bitemporal hemianopia (vision is missing in the outer half of both the right and left visual field) is ascribed to chiasmal compression, as can be seen in the setting of a pituitary mass or large suprasellar aneurysm. This particular defect is hypothesized to be from compression of the decussating nasal fibers at the central chiasm (which receive input from the temporal field, as shown in Fig 1). The temporal fibers remain uncrossed at the chiasm and, therefore, are unaffected.[6] Associated findings in patients with a sellar and/or suprasellar lesion can include EOM dysfunction related to cavernous sinus invasion by the lesion, causing compression of the transiting cranial nerves (CN), such as in the patient with a pituitary macroadenoma described in Fig 7. At MR imaging, uncomplicated pituitary macroadenoma will be T1 and T2 isointense, with moderate-to-bright enhancement after contrast administration, which will lag behind the enhancement of the normal pituitary tissue on dynamic imaging.[11] Gradient echo imaging assists in evaluation for hemorrhage associated with the lesion.[12]

Retrochiasmal lesions result in contralateral homonymous field defects (either hemianopia or quadrantanopia). If the hemianopia is complete, then further localization is not possible clinically, which provides an opportunity for the radiologist to aid in diagnosis. CT may be used in the acute setting if there is concern for ischemic stroke or hemorrhage and MR imaging performed to provide increased specificity and if there is concern for underlying mass or infection. Lesions that could result in binocular homonymous field defects with injury to the retrochiasmal visual pathway include posterior cerebral artery territory ischemia, venous sinus thrombosis with venous ischemic injury, head trauma, neoplasm, abscess, hemorrhage, demyelinating disease, or degenerative disorders such as Alzheimer disease or posterior cortical atrophy.[6]

Vascular ischemia is a common cause of binocular vision loss, with cortical blindness that results from damage to the primary visual cortex in the occipital lobe, which is largely in the posterior cerebral artery territory. The size of the

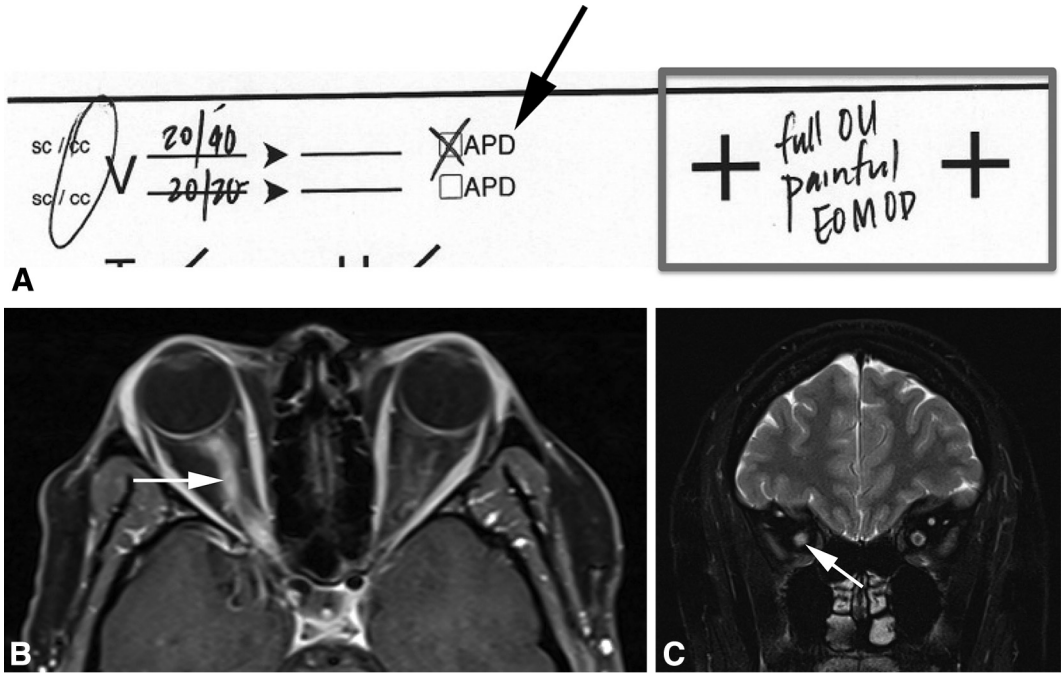

Fig 6. Optic neuritis. A 36-year-old woman presented to the emergency department with subjective loss of vision in the right eye on waking. *A*, Clinical findings for a patient with right eye optic neuritis include decreased visual acuity (20/40) and relative afferent pupillary defect (*arrow*), with painful extraocular motility (EOM) in the affected eye (OD) (box). *B*, Axial T1 fat-saturated postcontrast images demonstrate abnormal enhancement of the right optic nerve, intraconal (*arrow*) and intracanalicular segments. *C*, Coronal T2 fat-saturated image demonstrates abnormal increased signal intensity in the enlarged right optic nerve, indicative of edema (*arrow*).

visual field defect that results from ischemic damage to the primary visual cortex correlates to the size of the lesion itself and can range from a small scotoma (blind spot), to quadrantanopia (a fourth of the visual field is absent in both eyes), to hemianopia (a full hemifield defect in both eyes). Central vision may be spared (macular sparing) in anterior occipital lesions (supplied by middle cerebral artery) because the fovea is represented more posteriorly (supplied by the posterior cerebral artery). It thus is important to highlight that occipital cortex receives a blood supply from both the posterior and middle cerebral arteries.[13]

Patients with the rare clinical syndrome of posterior cortical atrophy, also known as Benson syndrome, will also have vision loss, such as the patient in Fig 8. On clinical examination, these patients can demonstrate relatively preserved visual acuity and a normal ophthalmologic structural examination; however, abnormalities will be uncovered during visual field testing. Benson syndrome is dominated by disruption of higher-order visual processes, with symptoms such as agnosia, apraxia, and simultagnosia, and is considered a variant of Alzheimer disease.[14,15] Patients with simultagnosia will describe objects, in this instance, the Ishihara color plates as "orange and green dots" (Fig 3) but are unable to "see the bigger picture" and name the number or symbol formed by the dots ("missing the forest for the trees"). This component of the neurologic condition is secondary to atrophy, which affects the visual association areas in the parietal and occipital lobes. Visual field deficit will be related to visual cortex atrophy.[16]

ANISOCORIA AND PUPILLARY DISORDERS

Ophthalmologic Examination

Assessing the pupils provides insight into complex neuronal circuitry that governs the pupillary response: afferent and efferent visual pathways as well as the autonomic nervous system (Fig 9*A*, -*B*). Pupillary dilatation is mediated by the sympathetic nervous system through a 3-neuron pathway: the first-order neuron originates at the hypothalamus and synapses at the ciliospinal center of Budge in the cervical spinal cord (C8–T2); the second-order neuron travels from the sympathetic trunk via the brachial plexus, over the lung apex, and ascends to the superior cervical ganglion (near the bifurcation of the common carotid artery); and the third-order neuron ascends with the internal carotid artery through the cavernous sinus to join CN V1 (ophthalmic division of the trigeminal nerve) to access the orbit via the superior orbital fissure and to travel to the dilator muscle (Fig 9*A*).[6]

Pupillary constriction is largely governed by the parasympathetic nervous system effect on the smooth-muscle fibers of the iris sphincter muscle. The Edinger-Westphal nucleus of the oculomotor complex contains parasympathetic preganglionic neurons that have axons that travel in the oculomotor nerve and that terminate in the ciliary ganglion. The ciliary ganglion is located behind the globe temporal to the ophthalmic artery. The parasympathetic postganglionic axons travel with the short ciliary nerve and end on the iris sphincter. The Edinger-Westphal nucleus re-

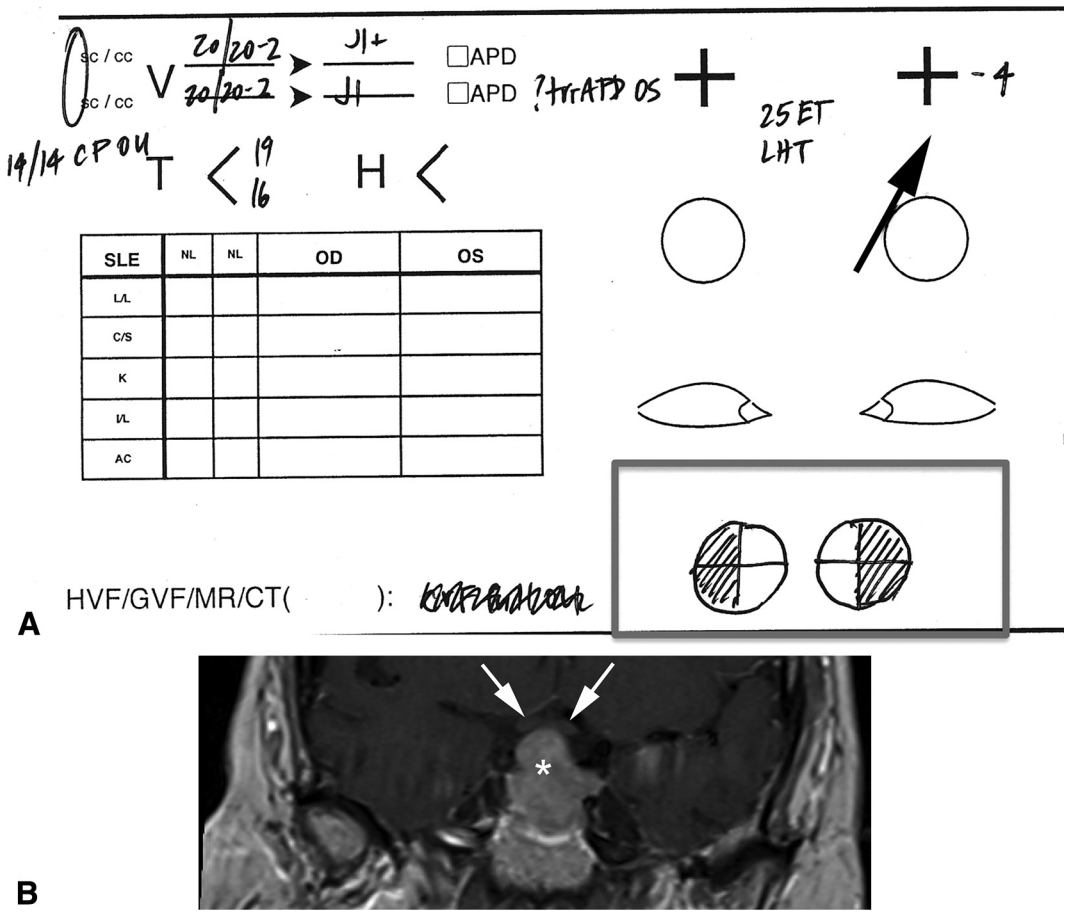

Fig 7. Pituitary macroadenoma. A 48-year-old woman with a history of chronic headache and blurry vision. *A*, Clinical examination findings in this patient demonstrate normal visual acuity, intraocular pressure (T values of 19 and 16 mm Hg) and color vision (14/14 CPOU - color plates both eyes), with left-sided motility deficits (*arrow*) denoted by esotropia (ET) and left hypertropia (LHT) (deviation measurements denoted in prism diopters), related to cavernous sinus (specifically with cranial nerve VI) involvement. A trace relative afferent pupillary defect is questioned on the left (trrAPD OS). Evaluation of visual fields demonstrates classic findings of bitemporal hemianopia (box). *B*, Coronal T1-weighted postcontrast MR image demonstrates an enhancing sellar and suprasellar lesion (*), consistent with pituitary macroadenoma, causing superior displacement of the optic chiasm and proximal extent of the cisternal segments of optic nerves bilaterally (*arrows*).

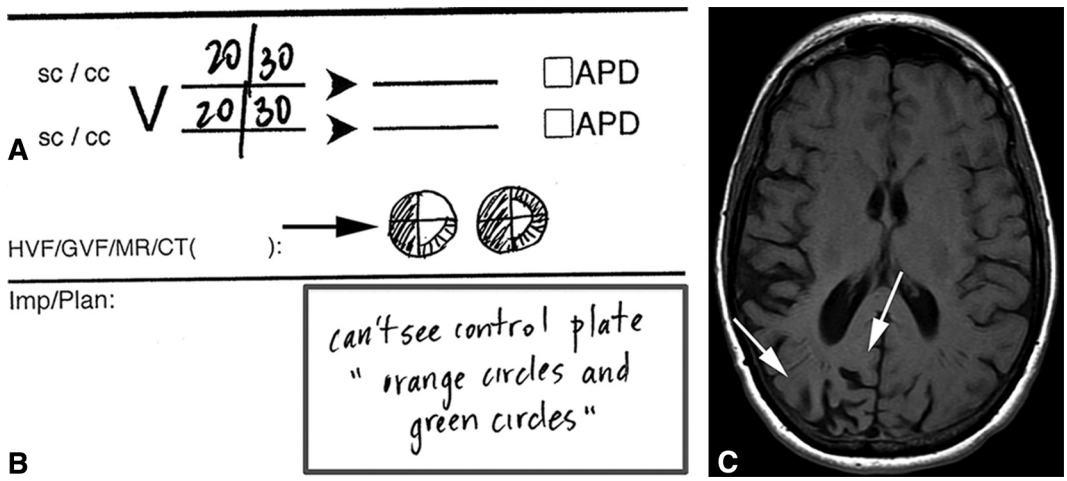

Fig 8. Benson syndrome. A 63-year-old woman presented with unexplained subjective vision loss for several months. *A*, The chart for this patient demonstrates relatively preserved visual acuity, measuring 20/30 bilaterally. *B*, In charting visual field defects, the visual fields are drawn as if looking through the patient's eyes (right eye on the right, left eye on the left). This image demonstrates bilateral visual field deficits (*shaded area*), including a left homonymous hemianopia (*arrow*). In addition, the patient described "orange and green dots" when shown the color plates but was unable to name the number or the symbol they formed, a condition known as simultagnosia (box). *C*, Axial T1-weighted MR images of the brain demonstrate subtle asymmetric, right (*arrows*) greater than left occipital lobe atrophy.

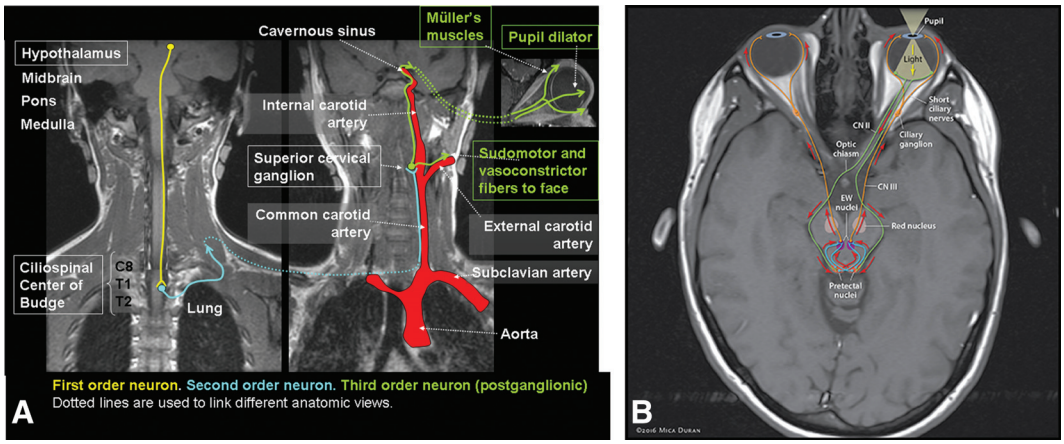

Fig 9. Basics of pupillary response. *A*, Sympathetic innervation originates in the hypothalamus, descends in the spinal cord to the ciliospinal center at approximately the C8 to T2 level, where second-order fibers then travel to the sympathetic chain and, subsequently, travel cranially to the superior cervical ganglion. Third-order neurons travel via the carotid plexus to the ophthalmic artery and first branch of CN V (ophthalmic division) to the eye. Used with the permission of Valerie Biousse, MD, and Nancy J. Newman, MD, and Thieme Publishing (Ref. 6, Fig 12.8). *B*, Parasympathetic innervation starts at the Edinger-Westphal (EW) nucleus near the oculomotor nerve nucleus and enters the orbit with CN III, synapsing at the ciliary ganglion and then traveling to the pupilloconstrictor muscles of the iris. When light is shined in the left eye, sensory information travels along the optic pathway to the left and right pretectal nuclei. The pretectal nuclei stimulate both left and right EW nuclei, from there, information travels through the left and right oculomotor nerves, causing both pupils to constrict. ©2016 Mica Duran. Printed with permission.

ceives sensory input from the optic nerve via the superior colliculus and pretectal area of the midbrain (Fig 9*B*).[6]

Pupils are assessed in light and dark conditions for size, shape, and reactivity by carefully comparing the 2 sides. A difference of >0.4 mm between the 2 pupils (anisocoria) is considered significant. The normal pupillary response is consensual: shining a light in one eye results in equal pupillary constriction of both eyes, with the degree of pupillary constriction being proportional to the brightness of the light source. When the pupillary response is asymmetric, a determination of whether the defect results from an abnormality of the afferent (optic nerve) or efferent (oculomotor nerve) pathway is necessary.

Analysis for a relative afferent system defect is performed by using the swinging flashlight test.[6] When a light is shined in the normal eye, both eyes briskly constrict. With unilateral optic nerve dysfunction, when the light is "swung" to the affected eye, the pupils "escape" or dilate because there is relatively decreased perceived light signal intensity (Fig 10). A lesion in the optic nerve or anterior visual pathway will result in an abnormal afferent pupillary response.[17] Obvious relative afferent pupillary defects are most commonly caused by optic neuropathies. Any large retinal lesion or severe central retinal lesion may also produce a less obvious relative afferent pupillary defect. If the pupillary defect is the result of an efferent abnormality, then the pupil remains unreactive to both direct and consensual light.[6]

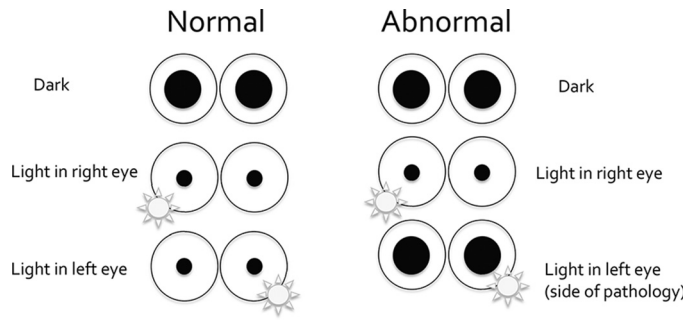

Fig 10. Swinging flashlight test. The normal pupillary response is consensual: shining a light in one eye results in pupillary constriction in both eyes (normal). The degree of pupillary constriction will be proportional to the brightness of the light source. With unilateral optic nerve dysfunction, the perceived light signal intensity is relatively less in the affected eye, so both pupils constrict less when the affected eye is stimulated (abnormal).

Imaging

Imaging coverage for patients with pupillary abnormalities will depend on whether or not the clinical suspicion is for a disorder of the parasympathetic or sympathetic pathway and if the abnormality is related to the afferent or efferent pathway. For afferent and efferent pupillary defects, imaging of the orbit, optic nerve, and brain stem is indicated. In the situation of sympathetic system abnormality, imaging coverage of the 3-neuron system would include the brain and orbits, cervical and upper thoracic cord, and the neck and upper chest.

If the patient has anisocoria, then etiologic considerations include Horner syndrome on the side of the smaller pupil, CN III palsy on the side of the larger pupil, or simply physiologic anisocoria.[17] Lesions along the sympathetic pathway to the eye can cause the clinical triad of miosis (constricted pupil), partial ptosis (drooping eyelid), and anhidrosis (loss of facial sweating) ipsilateral to the lesion location, a clinical triad known as Horner syndrome.[17] The classic clinical triad of ptosis, miosis, and anhidrosis is rare and can be quite subtle when present. Anhidrosis indicates a preganglionic lesion (first- or second- order neuron), whereas ipsilateral facial pain is suggestive of a third-order neuron lesion).[6]

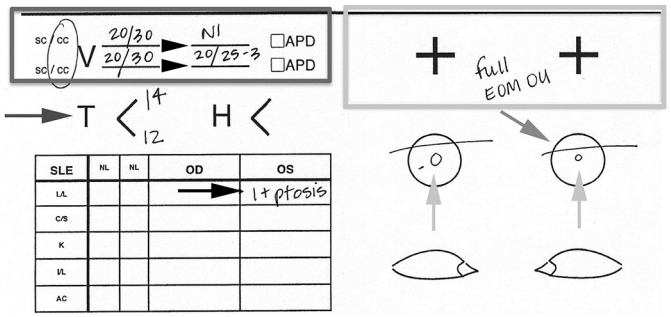

Fig 11. Horner syndrome. A 50-year-old man with new-onset left miosis, ptosis, and neck pain. An ophthalmology chart of this patient demonstrates near-normal visual acuity, with improvement in vision with pinhole indicative of a slight uncorrected refractive error (dark gray box), normal extraocular motility bilaterally (light gray box) and normal intraocular pressure bilaterally (*dark gray arrow*). Note is made of left-sided ptosis (*black arrow* to 1+ ptosis and *gray arrow* to graphic representation of lower lying left eyelid on the diagram) as well as asymmetrically decreased left pupil size, miosis (*light gray arrows* that point to the pupils drawn on the eye diagram).

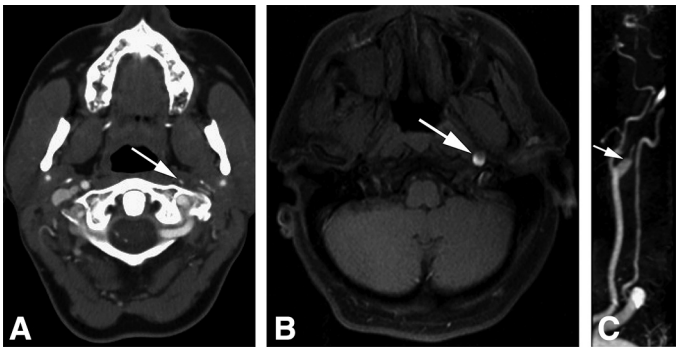

Fig 12. Horner syndrome secondary to left internal carotid artery dissection. *A*, CTA of the head and neck on vascular windows demonstrates minimal opacification of the left internal carotid artery (*arrow*). *B*, T1 fat-saturated MR image demonstrates abnormal increased signal intensity (methemoglobin) in the left internal carotid artery false lumen (*white arrow*). *C*, MR MIP image demonstrates a "string sign," with tapering and loss of more distal flow-related enhancement for the left internal carotid artery (*white arrow*).

Potential causes of Horner syndrome include first-order neuron lesions, such as hypothalamic or spinal cord tumors or demyelinating plaques; second-order neuron causes, such as trauma or tumor (including Pancoast tumor); and third-order neuron causes, such as internal carotid artery or cavernous sinus pathology.[6,18] Associated clinical features are often helpful in localizing the underlying cause and can help direct appropriate imaging; however, because pharmacologic testing can be incorrect and misleading, imaging of the entire sympathetic pathway is warranted if the accuracy of localization cannot be ensured[18] (Fig 9*A*).

A painful Horner syndrome is due to an arterial dissection until proved otherwise. CT or MR angiography is the imaging method of choice when evaluating for carotid dissection, with CT angiography holding the advantages of availability and decreased scan time.[19] The patient shown in Fig 11 presented with new-onset left miosis, ptosis, and neck pain. Other examination findings include near-normal visual acuity (improving with pinhole), normal extraocular motility, and normal intraocular pressure bilaterally. A note was made of left-sided ptosis (from denervation of the sympathetically controlled Müller muscle) and asymmetrically decreased left pupil size (from denervation of the iris dilator muscle). Of note, the difference in pupillary size is worse in the dark because the abnormal pupil does not dilate.[17] Vascular imaging in this patient demonstrated minimal opacification of the left internal carotid artery (Fig 12) in the setting of dissection.

DIPLOPIA AND DISORDERS OF THE EOMS

Ophthalmologic Examination

Extraocular motility can be recorded by a percentage of normal or on a scale from +1 through +4 for overaction and −1 through −4 for underaction, and is documented in each direction (up, down, right, left) from the examiner's perspective when looking at the patient. To test EOM function, the patient is requested to hold his or her head still and to follow the examiner's finger with the patient's eyes only in the various directions during assessment.

Understanding the innervation of the EOM can also provide clues for pattern recognition in instances in which the abnormal EOM function results from a cranial neuropathy. CN IV innervates the contralateral superior oblique muscle, which is responsible for intorsion and depression. CN VI innervates the ipsilateral lateral rectus muscle, which is responsible for abduction. CN III innervates the remaining ipsilateral EOMs, including the inferior rectus, medial rectus, superior rectus, inferior oblique as well as the levator palpebrae, the main muscle that elevates the upper eyelid.[2]

Imaging

MR imaging is the imaging method of choice to evaluate the CNs, with steady-state free precession sequences providing much higher spatial resolution to better depict these small intracranial structures.[19] Imaging coverage from the brain stem posteriorly to the orbit anteriorly will include the nuclei, course, and target muscles of CNs III, IV, and VI.[19] Pathology of the nerves themselves can result in abnormal extraocular motility, such as in the patient in Fig 13, with a CN III schwannoma. CN III schwannomas are rare overall but represent the most common of the pure motor nerve schwannoma.[15]

Abnormalities of EOM movement can also be seen in the setting of traumatic orbital fractures, with herniation of the EOMs through the fracture defect. Patients may report diplopia secondary to disconjugate gaze, and abnormalities of muscle movement can be appreciated on clinical examination. CT is the imaging technique of choice for assessment of the bony orbit. For orbital floor and medial orbital wall fracture, the position and shape of the inferior and medial rectus muscles, respectively, must be assessed to evaluate for possible entrapment. If the muscles remain flat in cross-section and in the correct position, then the fascia is likely

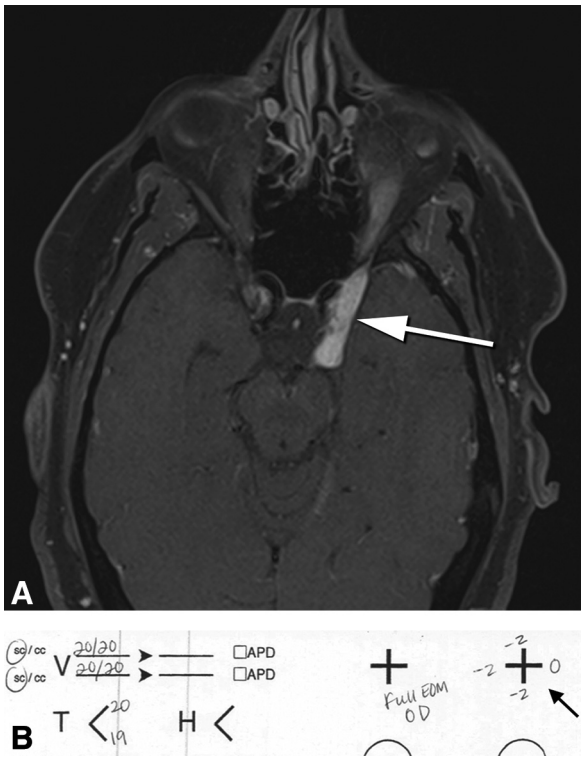

Fig 13. CN III schwannoma. *A*, An axial T1 postcontrast fat saturated image at the level of the cavernous sinus shows an enhancing lesion (*arrow*) along the oculomotor nerve. *B*, Charting of EOM motility (EOM) shows decreased eye movement of weakened adduction, elevation, and depression (*arrow* to the EOM assessment for the left eye with −2 scores). Normal intraocular pressure, normal EOM OD (right eye), and normal, uncorrected visual acuity are also charted.

intact.[20] Orbital wall fractures can result in diplopia due to increased orbital volume and resultant retroposition of the ipsilateral globe.[20]

Orbital space-occupying masses and masslike lesions, including thyroid orbitopathy, cellulitis, sarcoid, lymphoma, metastatic disease, and idiopathic orbital inflammation can also result in abnormalities of EOM movement due to direct involvement of the muscles by the disease process.[13] These processes can often be differentiated based on radiographic characteristics along with clinical evaluation.

ABNORMAL GLOBE POSITION

Ophthalmologic Examination

Globe position is measured by using the Hertel exophthalmometer. The base is the distance between the lateral canthi, and the corneal apex of each eye is recorded separately (Fig 14). Clinically, normal measurements are between 12 and 21 mm; however, up to 24 mm can be considered normal in African Americans.[21] A difference of >2 mm between the eyes is considered significant and warrants further evaluation.

Imaging

In most instances, imaging workup of proptosis begins with MR imaging of the orbits and the globe position can

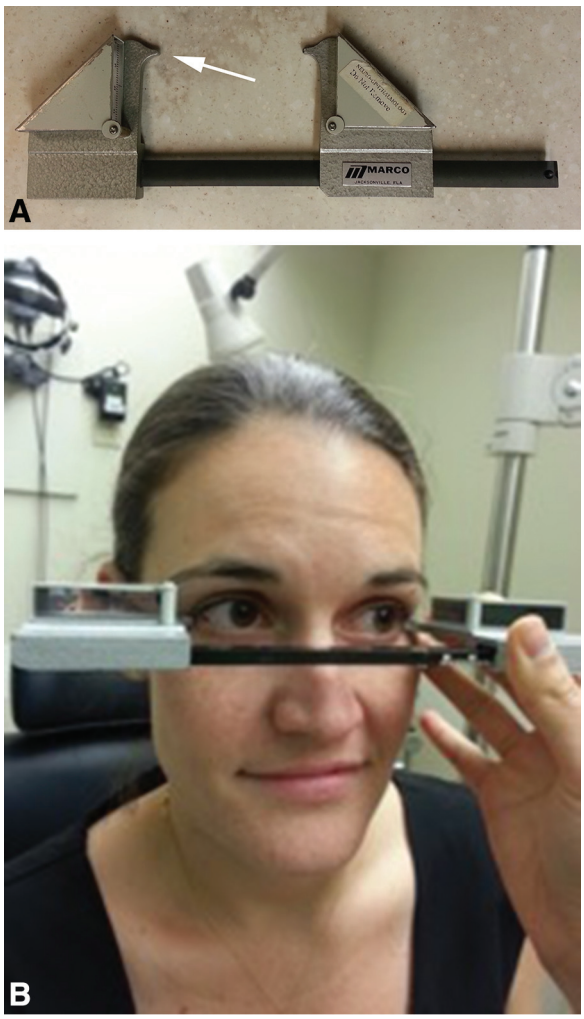

Fig 14. Hertel exophthalmometer. *A* and *B*, To use, each of the index points (*arrow*) are positioned at the lateral orbital walls. Measurements are taken by using a mirror marked in millimeters.

be measured on imaging examinations. To do so, a reference line is drawn between the anterior-most points of the bilateral zygomatic processes on axial imaging, known as the interzygomatic line (Fig 15). Globe protrusion by ≥21 mm beyond the interzygomatic line at the level of the lens is considered pathologic.[22] The differential diagnosis of proptosis is broad and includes orbital masses; vascular lesions and pathologies; space-occupying lesions, such as lymphoma, sarcoid, or idiopathic orbital inflammation; or EOM enlargement, which can be related to metastatic or infiltrative processes, for example, thyroid orbitopathy (Fig 15). Thyroid orbitopathy is the cause of unilateral proptosis in 15%–28% of adults and almost 80% of cases of bilateral proptosis.[23] If imaging is performed in the case of suspected thyroid orbitopathy, then CT is preferred because MR does not offer a significant advantage, except for cases in which evaluation of the optic nerve is warranted. EOM involvement tends to occur in a relatively systematic fashion, with the inferior rectus being the most commonly involved muscle.[24]

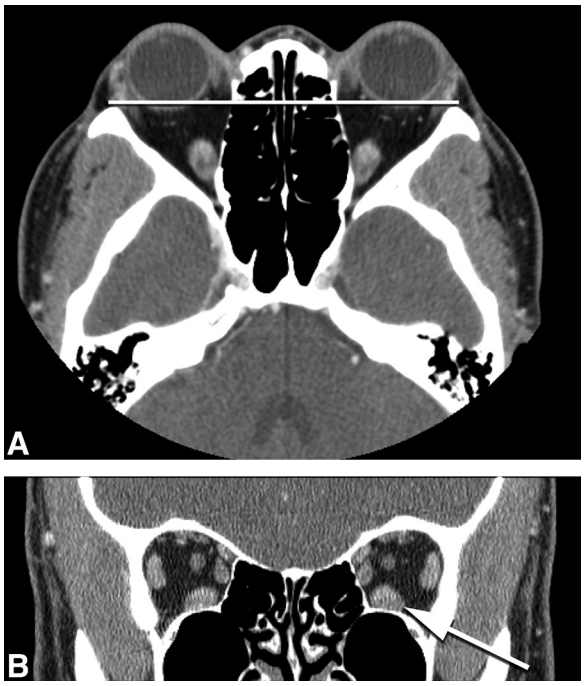

Fig 15. Measuring exophthalmos in thyroid orbitopathy. *A*, An axial noncontrast CT image at the level of the lens. Interzygomatic line is represented by the *white line*. *B*, A coronal CT image through the orbits shows bilateral particular enlargement of the inferior (*arrow* to the left inferior rectus) and lateral rectus muscles.

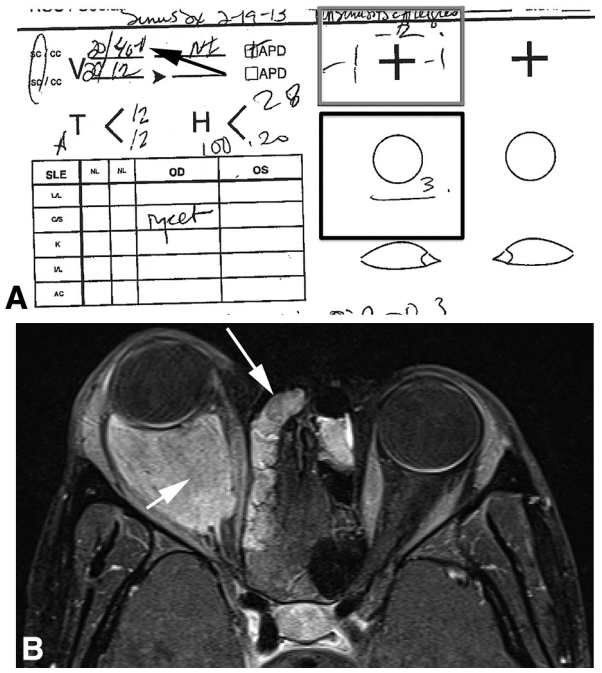

Fig 16. IgG4-related eye disease. A 15-year-old girl with 2 months of right eye proptosis. *A*, Physical examination findings in this patient include right eye: inferior scleral show (black box with grade 3 scleral exposure) as well as decreased visual acuity (*arrow*), an afferent pupillary defect (APD box marked), injected cornea/sclera (as written on the C/S line under the OD column for the SLE examination), and decreased extraocular motility (gray box showing −1 for adduction and abduction and −2 for elevation). *B*, Axial T1-weighted postcontrast fat-saturated MR image of the orbits demonstrates abnormal enhancing soft-tissue occupying the intraconal orbit (*short white arrow*), resulting in right-sided exophthalmos in this patient with biopsy-proved IgG4-related orbitopathy. The right ethmoid air cells are also partly filled (*long white arrow*) by abnormal soft tissue.

In patients with corkscrew episcleral blood vessels, in association with conjunctival chemosis, and pulsatile proptosis, a cavernous carotid fistula should be excluded. Cavernous carotid fistula can be traumatic or spontaneous, and can be supplied directly by the internal carotid artery, indirectly by branches of the internal or external carotid artery, or both.[25] CT angiography is more sensitive for detection of an cavernous carotid fistula than MR angiography, although both demonstrate similar findings of enlarged cavernous sinus, enlarged superior ophthalmic vein, proptosis, and enlargement of the EOMs.[26] Digital subtraction angiography is required for definitive diagnosis of cavernous carotid fistula.[25]

The clinical findings in a young patient who presented with a 2-month history of right eye proptosis are demonstrated in Fig 16, found to be secondary to IgG4 related orbitopathy. IgG4-related disease is a systemic inflammatory process of unknown etiology that can involve multiple different organs and organ systems. In the orbit, differentiating this process from other causes of orbital inflammation and/or infiltration of orbital soft tissues can be challenging. IgG4-related orbitopathy has been shown to involve the EOMs, the lacrimal gland, and the infraorbital nerve. The most common presenting symptoms are proptosis and/or periorbital swelling. MR imaging is the imaging technique of choice to better delineate the extent of disease. The most common imaging findings are infiltration of the EOMs, sparing the tendons (similar to thyroid eye disease), although the most frequently involved muscle is the lateral rectus (in contradistinction to thyroid eye disease, which preferentially affects the inferior rectus).[27]

Of note, in the evaluation of potential exophthalmos, it is important to consider which eye is abnormal because there is the possibility of one eye appearing proptotic, when in fact that eye is normal and the other eye is enophthalmic. Enophthalmos is the posterior displacement of the globe within the orbit, and, when unilateral, a difference of >2 mm is considered diagnostic. Causes of enophthalmos include any cause of increased orbital volume, such as facial trauma with orbital blow-out type fractures or silent sinus syndrome. In these examples, the globe "sinks" within the expanded cavity.[28] A sinister cause of enophthalmos is metastatic breast cancer, the most common metastatic lesion to the soft tissues of the orbit. Enophthalmos results secondary to the scirrhous reaction to the lesion, as shown in Fig 17.[1]

PAPILLEDEMA, INTRAOCULAR MASSES, INFECTION, OR HEMORRHAGE

Ophthalmologic Examination

The anterior segment can be evaluated by slit lamp examination (SLE). It contains the structures anterior to the vit-

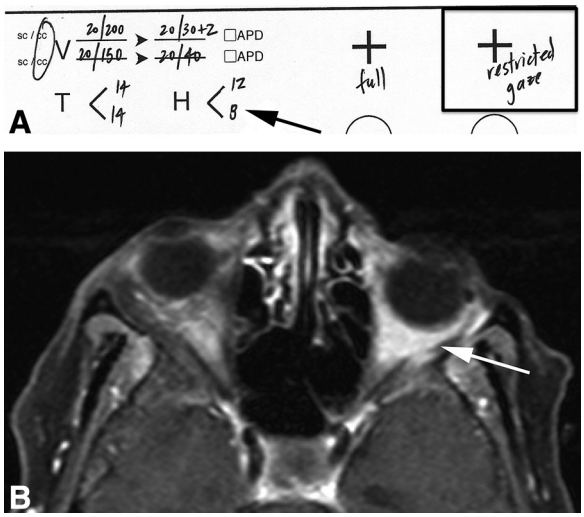

Fig 17. Metastatic breast cancer. A 76-year-old woman with known metastatic breast cancer and diplopia. *A*, On physical examination, this patient had left eye enophthalmos, measured by using a Hertel exophthalmometer (*arrow*) and restricted gaze, with abnormal EOM function in the left eye (box). *B*, An axial T1-weighted fat-saturated postcontrast MR image demonstrates abnormal enhancing soft tissue posterior to the globe in the left orbit (*arrow*) with scirrhous retraction and resultant left eye enophthalmos.

reous humor (lids, conjunctiva and sclera, cornea, iris, ciliary body, and lens), the anterior chamber (between the cornea and the iris) and the posterior chamber (the narrow space between the iris and the vitreous). A representative example of an SLE charting template is included in Fig 2, with examples of abnormal findings charted in Figs 11 and 16. Common abbreviations in the anterior segment examination are also included in Table 1. Pathology appreciated in the anterior segment is readily evaluated in the ophthalmologist's office by the SLE and rarely requires further evaluation by imaging. If anterior segment pathology precludes evaluation of the posterior segment, such as in the setting of hyphema, then imaging may be warranted to evaluate the globe and the orbit.

The fundoscopic examination evaluates the vitreous, optic disc, cup-to-disc ratio (c/d), macula, vasculature, and the periphery. In adult patients, proparacaine is commonly used to numb the eye, and 1% tropicamide and 2.5% phenylephrine are used to dilate the eye. Pupillary dilation cannot be performed if there is concern for narrow angles precipitating angle closure glaucoma or if there is a need to follow up serial pupillary examinations as part of the evaluation of neurologic status, such as in the setting of acute head injury or intracranial hemorrhage. The fundoscopic examination is most commonly documented with drawings that represent the findings on 2 circle templates. Intraocular masses can be detected at fundoscopy; however, imaging is commonly warranted to evaluate for orbital involvement and the extent of disease.

Imaging

Although CT is especially useful in assessment of osseous or calcified lesions, MR imaging, with its inherently superior

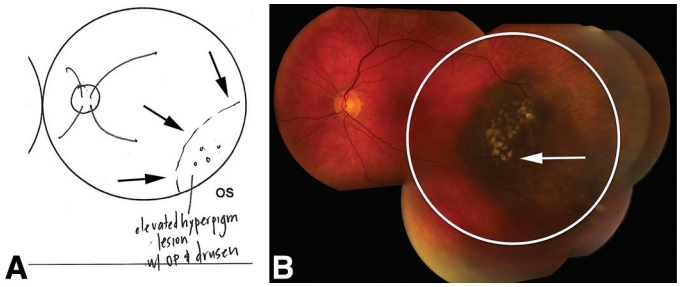

Fig 18. Ocular melanoma. *A*, An ophthalmology chart in a patient with left ocular melanoma includes a description of an elevated, hyperpigmented lesion with orange pigment (OP) and drusen (*arrows*). *B*, A fundoscopic image in this patient demonstrates the elevated and hyperpigmented lesion on the retina (*circle*), with orange pigment and drusen (*arrow*).

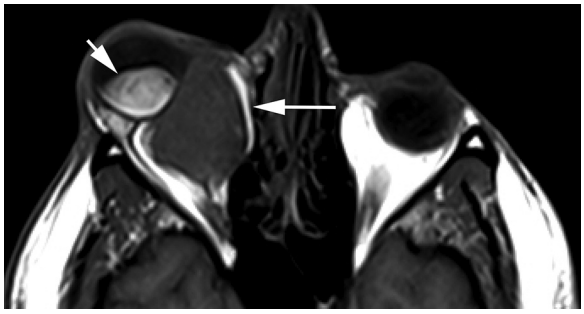

Fig 19. Ocular and extraocular melanoma. A 58-year-old man with vision loss and progressive enlargement and "discomfort of the right eye." An axial T1 precontrast MR image through the orbits demonstrates an intraocular T1 hyperintense mass arising from the uvea of the right globe (*short white arrow*). In addition, an intermediate signal intensity extraocular/intraorbital bulky mass is present (*long white arrow*). The patient underwent enucleation with pathology consistent with mixed cell type malignant melanoma with pigmented intraocular portion (T1 high signal intensity) and nonpigmented (amelanotic) extraocular/intraorbital portion (T1 intermediate signal intensity), which accounts for the complex imaging appearance.

soft-tissue contrast, is often the first imaging tool used in the evaluation of a patient with an ocular mass. In the patient in Fig 18, with orbital melanoma, an intraocular mass is seen fundoscopically and is drawn and charted accordingly. In a similar patient (Fig 19), also with orbital melanoma, an intraocular mass is appreciated; however, MR imaging demonstrates additional extra- and/or intraorbital components. On MR imaging, melanotic melanoma will display intrinsic T1 and T2 shortening effects of melanin that result in increased T1 and decreased T2 signal intensity.[1] Approximately 20% of melanomas are amelanotic and will lack these characteristic imaging findings (Fig 19).[29] MR is also helpful in evaluating for tumor size, extraocular extension (Fig 19), and ciliary body infiltration, all of which are associated with a worse prognosis.[29]

Intraocular hemorrhage can also be diagnosed fundoscopically and, in some instances, does not require imaging for further workup. These hemorrhages are indicators of underlying systemic or ocular diseases and can occur on the surface of the retina (preretinal), in the retina itself (flame-shaped or dot-and-blot hemorrhage), or beneath the retina (subretinal). The specific location of

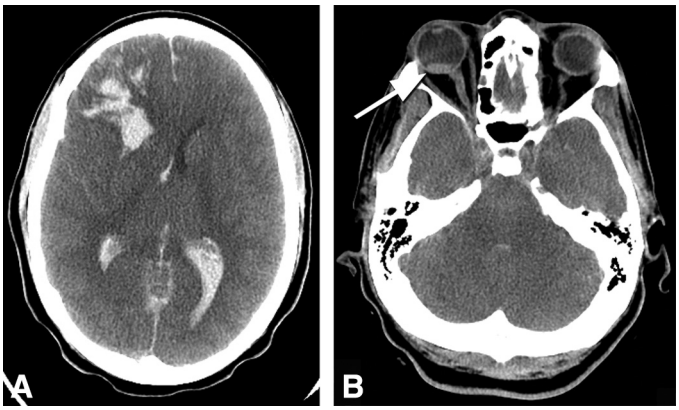

Fig 20. Intraparenchymal hemorrhage. A 48-year-old man found unresponsive. *A*, An axial CT image through the head demonstrates extensive multicompartmental hemorrhage, with large right frontal intraparenchymal hemorrhage and intraventricular extension. *B*, An axial CT image through the orbits in the same patient demonstrates extension of subarachnoid hemorrhage along the right optic nerve sheath with associated vitreous hemorrhage (*arrow*), consistent with Terson syndrome.

the hemorrhage is often associated with a characteristic appearance on fundoscopy. Diabetic retinopathy is often associated with intraretinal (dot-and-blot) and preretinal hemorrhages. Flame-shaped hemorrhages occur in hypertensive retinopathy and vein occlusion. Rupture of superficial retinal vessels can also be seen in hypertension and trauma. These preretinal hemorrhages may rupture into the vitreous.[30]

Terson syndrome is ocular hemorrhage due to subarachnoid hemorrhage, with an incidence of up to 46% in patients with subarachnoid hemorrhage. Terson syndrome is associated with more severe subarachnoid hemorrhage and with a higher mortality.[31] The ocular hemorrhage is not an extension of the intracranial blood products but rather represents the sequelae of the sudden increase in intracranial pressure associated with the subarachnoid hemorrhage. This results in rupture of retinal venules and subsequent preretinal bleeds, and leads to accumulation of blood products in the vitreous.[23] In Fig 20, a noncontrast CT of the head demonstrates the typical findings of multicompartmental hemorrhage, including subarachnoid hemorrhage. On the fundoscopic examination, multifocal preretinal hemorrhage can be seen and is described in the chart through diagrams (Fig 21).

Patients who are immunocompromised can develop severe ocular infections, such as chorioretinitis (infection or inflammation of the choroid and retina, and a form of posterior uveitis), which can be appreciated on fundoscopic examination (Figs 22 and 23). These infections are commonly due to toxoplasmosis or cytomegalovirus but may also be secondary to tuberculosis, syphilis, herpes simplex virus, or varicella.[32] Imaging in these patients is not always pursued; however, MR imaging may be indicated in the presence of clinical optic nerve involvement and can evaluate the extent of disease and involvement of other orbital or intracranial structures.[33]

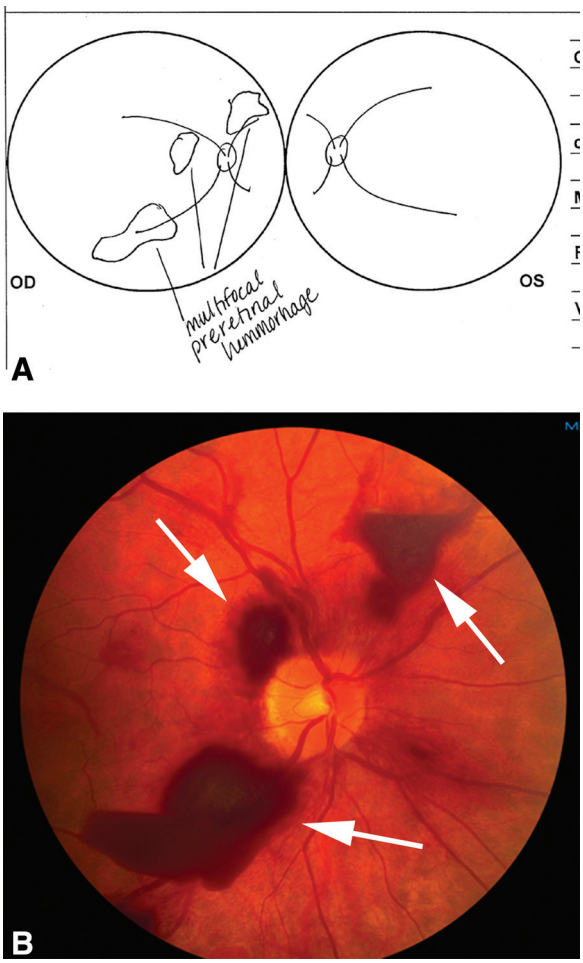

Fig 21. Terson syndrome. *A*, An ophthalmology chart of fundoscopic examination recording multifocal preretinal hemorrhage. *B*, A fundoscopic image in the same patient, demonstrates multifocal preretinal hemorrhage (*arrows*).

At the fundoscopic examination, an ophthalmologist can describe "disc edema," with associated findings of blurred disc margins, elevation of the optic nerve head, and obscuration of the vessels (Fig 24). Cotton-wool spots and hemorrhages may be seen in more severe cases. Papilledema is the term reserved to describe disc edema in the setting of proved elevated intracranial pressure as determined by ventricular or lumbar puncture measurements.[15] In the setting of disc edema identified by the ophthalmologist, evaluation of intracranial contents with CT or MR imaging is necessary to evaluate for potential causes, such as hydrocephalus, CNS infection, and mass as well as to look for additional signs of increased intracranial pressure. CT and MR imaging can show findings associated with idiopathic intracranial hypertension, including prominent CSF spaces around the optic nerves, flattening of the posterior globe, partially empty sella turcica, and transverse sinus stenosis. Although these findings may be indicative of increased intracranial pressure, none are pathognomonic for idiopathic intracranial hypertension, and all have been observed in subjects who are presumably normal.[34]

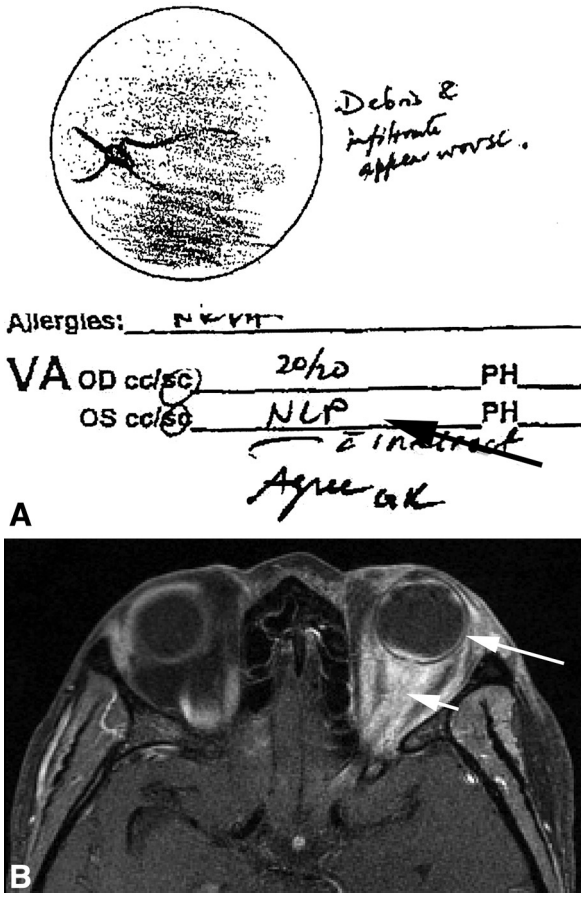

Fig 22. Endophthalmitis. A 30-year-old woman with HIV and unknown CD4 count, with vision loss and left eye pain. *A*, A diagram from a follow-up visit fundoscopic examination demonstrates worsening debris and infiltrate. Visual acuity in the left eye is recorded at no light perception (NLP) (*arrow*). *B*, Axial T1-weighted fat-saturated postcontrast MR image demonstrates abnormal enhancement that involves the left globe (*long white arrows*) and extending into the optic nerve (*short white arrow*), consistent with chorioretinitis and optic neuritis.

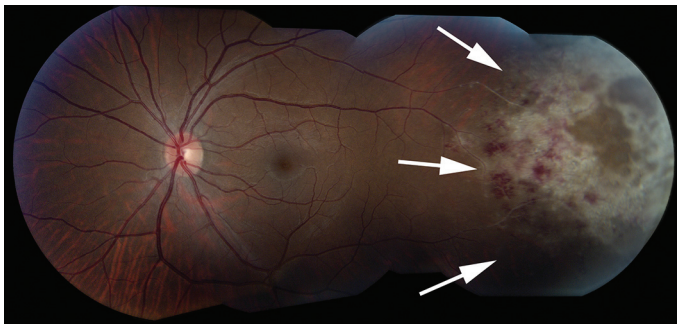

Fig 23. Retinitis. Fundoscopic images from a different patient, with less-severe disease demonstrate diffuse fluffy retinal whitening, with associated retinal hemorrhages (*arrows*).

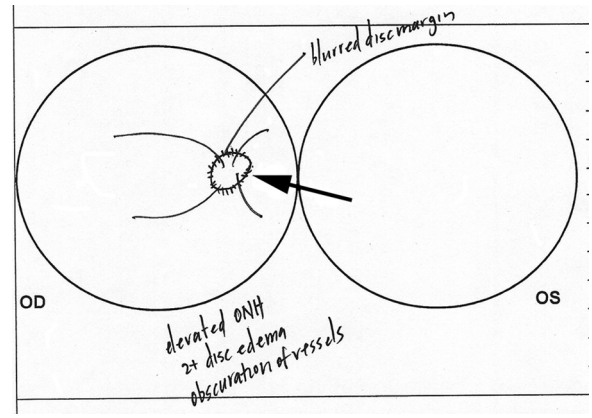

Fig 24. Disc edema. A 45-year-old woman who presented with headache and blurry vision (only right eye findings were charted). Ophthalmology chart of the fundoscopic examination in this patient demonstrates blurring of the disc margin (*arrow*), elevated optic nerve head (ONH), disc edema, and obscuration of vessels.

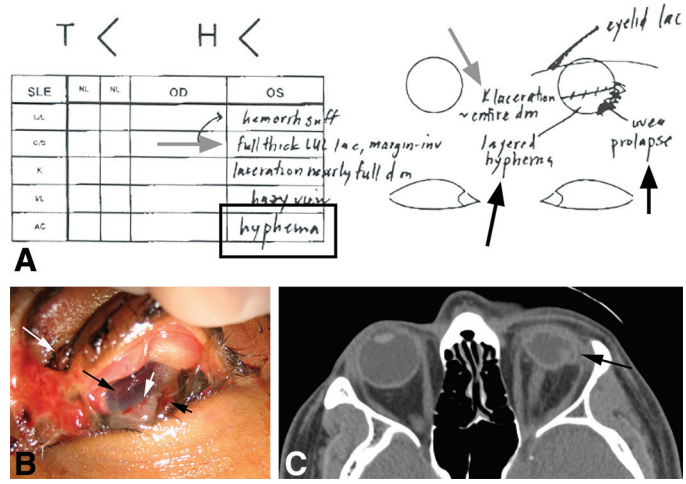

Fig 25. An open globe. A 38-year-old man with severe facial trauma and immediate vision loss, with an open globe on clinical examination. *A*, Chart documentation of SLE findings in the left eye (OS) shows: left upper lid laceration (*long oblique line* marked "eyelid lac"), corneal laceration (*gray arrow* marked "K laceration≈ entire diameter ["dm"]), hyphema (*long black line* marked: layered hyphema and charted in black box, on the row AC, as hyphema), and uveal prolapse (*short black arrow*). *B*, Photograph, demonstrating the examination findings described above: full-thickness left upper lid laceration (*long white arrow*), corneal laceration that involves the entire diameter of the cornea (*long black arrow*), layered hyphema (*short white arrow*), and uveal prolapse (*short black arrow*). *C*, An axial CT image through the globes demonstrates severe left globe deformity, ie, "flat tire" sign (*arrow*).

OCULAR TRAUMA

Ophthalmologic Examination

Open globe injuries can be classified as an open globe rupture, which results from blunt injury and occurs at the site of the greatest structural weakness, typically the equator, or as an open globe laceration, which results from penetrating trauma by a sharp object or projectile.[35] This type of injury constitutes an ophthalmologic emergency and is managed with surgery for primary repair. If a full-thickness defect is found clinically, with or without prolapse of intraocular contents, then the diagnosis of an open globe can be made. Clinical examination can also assess additional traumatic injuries, such as lid laceration, corneal laceration, hyphema, and uveal prolapse (Fig 25). Immediate complications of an open globe can include vision loss and endophthalmitis.

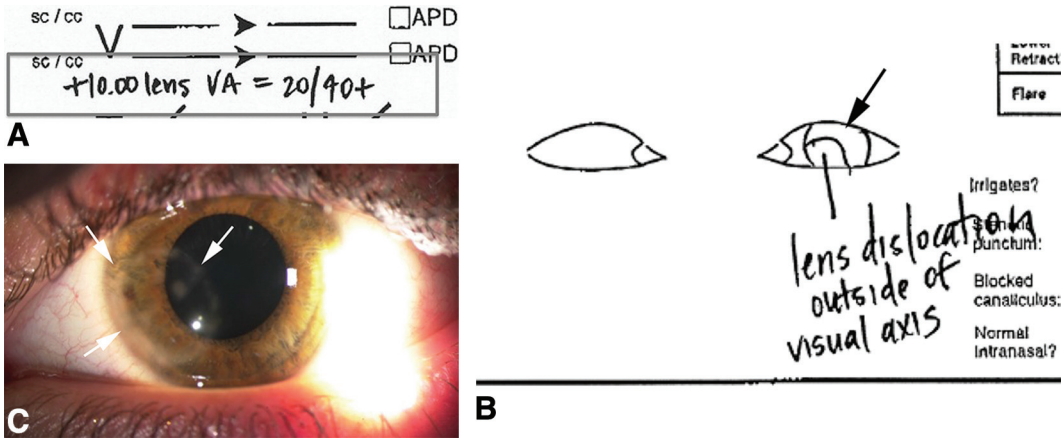

Fig 26. Lens dislocation in the setting of Marfan disease. *A*, In the ophthalmology note, visual acuity (VA) is recorded as 20/40+, with assistance of a +10.00 lens on the left eye (box). *B*, The ophthalmologist also notes a left eye lens dislocation out of the visual axis (*arrow*). *C*, A clinical photograph in the patient charted above demonstrates the lens dislocated from the visual axis (*arrows*).

Sympathetic ophthalmia is an unusual complication, which can be seen months to years after a unilateral open globe injury (or surgery or penetrating trauma) and results in bilateral chronic progressive vision loss due to diffuse granulomatous intraocular uveal inflammation.[36,37]

Imaging

CT is the test of choice in the setting of trauma because it is readily available, fast, and effective to screen for globe injury, traumatic lens displacement, radiopaque foreign objects, and osseous injury.[35] In the absence of clinical examination and history, the sensitivity and specificity of CT for detecting an open globe is 75% and 93%, respectively. The positive predictive value is 95%.[38] In a patient with decreased visual acuity and trauma, the radiologist should evaluate for an open globe injury, defined as any full-thickness injury to the cornea, sclera, or both. CT findings of an open globe include abnormal globe contour, loss of globe volume, "flat tire" sign, scleral discontinuity, intraocular air, or intraocular foreign body.[19] Another sign of an open globe injury is "deepening" of the anterior chamber, which occurs when there is disruption of the posterior sclera, which results in decompression of the vitreous and retropulsion of the lens.[39] The radiologist can provide additional insight to prognosis because imaging findings of distortion of the vitreous, lens disruption, and vitreous hemorrhage are associated with poor visual outcomes.[38]

Trauma patients may also experience traumatic lens dislocations. Blunt trauma to the eye deforms the globe, which results in stretching or possibly tearing of the zonular ligaments that hold the lens in place. The lens can dislocate anteriorly into the anterior chamber or, more commonly, posteriorly into the posterior segment, which results in decreased visual acuity.[2,20] Lens dislocation can also occur in the setting of connective tissue disorders, including Marfan syndrome, as pictured in Fig 26, with bilateral lens dislocations; in the absence of significant trauma, patients should be evaluated for an underlying systemic process, such as Marfan syndrome, homocystinuria, and Ehlers-Danlos syndrome.[20] Because lens dislocation is rarely complete, it can typically be directly visualized on dilated SLE, as in the patient in Fig 26. If the lens is completely dislocated, then the lens may be appreciated at indirect ophthalmoscopy.[40]

CONCLUSION

The radiologist is better equipped to accurately select the protocol and interpret studies when possessing an understanding of the information available in the ophthalmology clinic note. Orbital and visual pathway pathologies usually result in readily detectable symptoms, which can direct the evaluating clinician toward a specific etiology or diagnosis. When confirmatory imaging studies are necessary to identify a more definite cause for the clinical findings or to confirm a suspected diagnosis, being able to decipher complicated handwritten, and sometimes hand-drawn, ophthalmology notes aid the interpreting radiologist in reaching a more appropriate and succinct differential diagnosis.

ACKNOWLEDGMENTS

We thank Eric Jablonowski, Kevin Makowski, and Mica Duran for the assistance in the preparation of our figures. We also thank Nancy Newman, MD, and Valérie Biousse, MD, and Thieme Publishing for permission to use Figs 1 and 9*A*.

REFERENCES

1. Tailor TD, Gupta D, Dalley RW, et al. **Orbital neoplasms in adults: clinical, radiologic, and pathologic review.** *RadioGraphics* 2013;33:1739–58. 10.1148/rg.336135502
2. Kels BD, Grzybowski A, Grant-Kels JM. **Human ocular anatomy.** *Clin Dermatol* 2015;33:140–46. 10.1016/j.clindermatol.2014.10.006
3. Lee AG, Brazis PW, Garrity JA, et al. **Imaging for neuro-ophthalmic and orbital disease.** *Am J Ophthalmol* 2004;138:852–62. 10.1016/j.ajo.2004.06.069
4. Levenson JH, Kozarsky A. **Visual acuity change.** In: Walker HK, Hall WD, Hurst, JD. *Clinical Methods: The History, Physical, and Laboratory Examinations*. 3rd ed. Boston: Butterworths; 1990:553–555

5. Simunovic MP. **Acquired color vision deficiency.** *Surv Ophthalmol* 2016;61:132–55. 10.1016/j.survophthal.2015.11.004
6. Biousse V, Newman NJ. *Neuro-Ophthalmology Illustrated*. New York: Thieme Medical Publishers; 2015
7. Germann CA, Baumann MR, Hamzavi S. **Ophthalmic diagnoses in the ED: optic neuritis.** *Am J Emerg Med* 2007;25:834–37. 10.1016/j.ajem.2007.01.021
8. Ebers GC. **Optic neuritis and multiple sclerosis.** *Arch Neurol* 1985;42:702–04. 10.1001/archneur.1985.04060070096025
9. Optic Neuritis Study Group. **Multiple sclerosis risk after optic neuritis: final optic neuritis treatment trial follow-up.** *Arch Neurol* 2008;65:727–32. 10.1001/archneur.65.6.727
10. LeBedis CA, Sakai O. **Nontraumatic orbital conditions: diagnosis with CT and MR imaging in the emergent setting.** *Radiographics* 2008;28:1741–53. 10.1148/rg.286085515
11. Miki Y, Matsuo M, Nishizawa S, et al. **Pituitary adenomas and normal pituitary tissue: enhancement patterns on gadopentetate-enhanced MR imaging.** *Radiology* 1990;177:35–38. 10.1148/radiology.177.1.2399335
12. Tosaka M, Sato N, Hirato J, et al. **Assessment of hemorrhage in pituitary macroadenomas by T2*-weighted gradient-echo MR imaging.** *AJNR Am J Neuroradiol* 2007;28:2023–29. 10.3174/ajnr.A0692
13. Melnick MD, Tadin D, Huxlin KR. **Re-learning to see in cortical blindness.** *Neuroscientist* 2016;22:199–212. 10.1177/1073858415621035
14. Benson DF, Davis RJ, Snyder BD. **Posterior cortical atrophy.** *Arch Neurol* 1988;45:789–93. 10.1001/archneur.1988.00520310107024
15. Osborne, AG. *Osborne's Brain: Imaging, Pathology, and Anatomy*. Salt Lake City: Amrysis; 2013
16. Tang-Wai DF, Graff-Radford NR, Boeve BF, et al. **Clinical, genetic, and neuropathologic characteristics of posterior cortical atrophy.** *Neurology* 2004;63:1168–74. 10.1212/01.WNL.0000140289.18472.15
17. Kardon, R. **The pupils and accommodation.** In: Albert DM, Miller JW, Azar DT. Albert & Jakobiec's Principles & Practice of Ophthalmology. 3rd ed. Philadelphia: Saunders; 2008:4029–48
18. Walton KA, Buono LM. **Horner syndrome.** *Curr Opin Ophthalmol* 2003;14:357–63. 10.1097/00055735-200312000-00007
19. Sheth S, Branstetter BF IV, Escott EJ. **Appearance of normal cranial nerves on steady-state free precession MR images.** *Radiographics* 2009;29:1045–55. 10.1148/rg.294085743
20. Kubal WS. **Imaging of orbital trauma.** *Radiographics* 2008;28:1729–39. 10.1148/rg.286085523
21. Migliori ME, Gladstone GJ. **Determination of the normal range of exophthalmometric values for black and white adults.** *Am J Ophthalmol* 1984;98:438–42. 10.1016/0002-9394(84)90127-2
22. Hilal SK, Trokel SL. **Computerized tomography of the orbit using thin sections.** *Semin Roentgenol* 1977;12:137–47. 10.1016/0037-198X(77)90015-3
23. Shaw HE Jr, Landers MB. **Vitreous hemorrhage after intracranial hemorrhage.** *Am J Ophthalmol* 1975;80:207–13. 10.1016/0002-9394(75)90134-8
24. Parmar H, Ibrahim M. **Extrathyroidal manifestations of thyroid disease: thyroid ophthalmopathy.** *Neuroimaging Clin N Am* 2008;18:527–36. viii–ix
25. Winegar BA, Gutierrez JE. **Imaging of orbital trauma and emergent non-traumatic conditions.** *Neuroimaging Clin N Am* 2015;25:439–56. 10.1016/j.nic.2015.05.007
26. Chen CC, Chang PC, Shy CG, et al. **CT angiography and MR angiography in the evaluation of carotid cavernous sinus fistula prior to embolization: a comparison of techniques.** *AJNR Am J Neuroradiol* 2005;26:2349–56
27. Tiegs-Heiden CA, Eckel LJ, Hunt CH, et al. **Immunoglobulin G4-related disease of the orbit: imaging features in 27 patients.** *AJNR Am J Neuroradiol* 2014;35:1393–97. 10.3174/ajnr.A3865
28. Hamedani M, Pournaras JA, Goldblum D. **Diagnosis and management of enophthalmos.** *Surv Ophthalmol* 2007;52:457–73. 10.1016/j.survophthal.2007.06.009
29. Lemke AJ, Hosten N, Bornfeld N, et al. **Uveal melanoma: correlation of histopathologic and radiology findings by using thin-section MR imaging with a surface coil.** *Radiology* 1999;210:775–83. 10.1148/radiology.210.3.r99fe39775
30. Kaiser PK, Neil JF, Pineda R. *Massachusetts Eye and Ear Infirmary Illustrated Manual of Ophthalmology*. 4th ed. London: Saunders; 2014
31. Hassan A, Lanzino G, Wijdicks EF, et al. **Terson's syndrome.** *Neurocrit Care* 2011;15:554–58. 10.1007/s12028-011-9555-2
32. Jabs DA. **Ocular manifestations of HIV infection.** *Trans Am Ophthalmol Soc* 1995;93:623–83
33. Moraes HV. **Ocular manifestations of HIV/AIDS.** *Curr Opin Ophthalmol* 2002;13:397–403. 10.1097/00055735-200212000-00010
34. Ridha MA, Saindane AM, Bruce BB, et al. **MRI findings of elevated intracranial pressure in cerebral venous thrombosis versus idiopathic intracranial hypertension with transverse sinus stenosis.** *Neuroophthalmology* 2013;37:1–6. 10.3109/01658107.2012.738759
35. Kuhn F, Morris R, Witherspoon CD, et al. **A standardized classification of ocular trauma.** *Ophthalmology* 1996;103:240–43. 10.1016/S0161-6420(96)30710-0
36. Rahman I, Maino A, Devadason D, et al. **Open globe injuries: factors predictive of poor outcome.** *Eye* 2006;20:1336–41. 10.1038/sj.eye.6702099
37. Arevalo JF, Garcia RA, Al-Dhibi HA, et al. **Update on sympathetic ophthalmia.** *Middle East Afr J Ophthalmol* 2012;19:13–21. 10.4103/0974-9233.92111
38. Joseph DP, Pieramici DJ, Beauchamp NJ. **Computed tomography in the diagnosis and prognosis of open-globe injuries.** *Ophthalmology* 2000;107:1899–906. 10.1016/S0161-6420(00)00335-3
39. Weissman JL, Beatty RL, Hirsch WL, et al. **Enlarged anterior chamber: CT finding of a ruptured globe.** *AJNR Am J Neuroradiol* 1995;16:936–38
40. Hardjasudarma M, Rivera E, Ganley JP, et al. **Computed tomography of traumatic dislocation of the lens.** *Emerg Radiol* 1994;1:180–81. 10.1007/BF02614922